

Efficient Manipulation-Enhanced Semantic Mapping With Uncertainty-Informed Action Selection

Nils Dengler

Jesper Mücke

Rohit Menon

Maren Bennewitz

Abstract—Service robots operating in cluttered human environments such as homes, offices, and schools cannot rely on predefined object arrangements and must continuously update their semantic and spatial estimates while dealing with possible frequent rearrangements. Efficient and accurate mapping under such conditions demands selecting informative viewpoints and targeted manipulations to reduce occlusions and uncertainty. In this work, we present a manipulation-enhanced semantic mapping framework for occlusion-heavy shelf scenes that integrates evidential metric-semantic mapping with reinforcement-learning-based next-best view planning and targeted action selection. Our method thereby exploits uncertainty estimates from the Dirichlet and Beta distributions in the semantic and occupancy prediction networks to guide both active sensor placement and object manipulation, focusing on areas of limited knowledge and selecting actions with high expected information gain. For object manipulation, we introduce an uncertainty-informed push strategy that targets occlusion-critical objects and generates minimally invasive actions to reveal hidden regions. The experimental evaluation shows that our framework highly reduces object displacement and drops while achieving a 95% reduction in planning time compared to the state-of-the-art, thereby realizing real-world applicability.

I. INTRODUCTION

The successful deployment of general-purpose service robots in human-centric environments, such as homes and offices, depends on their ability to perceive and manipulate diverse objects within cluttered and constrained spaces. In such environments, robots must not only go beyond traditional passive perception approaches, such as static mapping, but also extend conventional active perception methods [1] by integrating physical interactions with the environment [2]. This allows them to actively remove occlusions by physically uncovering hidden regions [3], [4], which is especially critical for tasks such as exploring unknown environments [5], constructing detailed object models [6], and locating objects obscured from direct view [7]. However, such manipulation actions come at a cost, as uninformed physical interactions often not only increase the uncertainty about the manipulated object’s pose and stability, but also of the other elements in the scene. Consequently, a key challenge in interactive perception is to select actions carefully, e.g., guided by uncertainty.

To tackle this challenge, predictive networks [8], [9] have been proposed to quantify the effect of pushing objects

All authors are with the University of Bonn, Germany. M. Bennewitz and N. Dengler are additionally with the Lamarr Institute for Machine Learning and Artificial Intelligence. M. Bennewitz and R. Menon are also with the Center for Robotics, Bonn, Germany. This work has partly been supported by the European Commission under grant agreement numbers 964854 (RePAIR) and by the BMBF within the Robotics Institute Germany, grant No. 16ME0999.

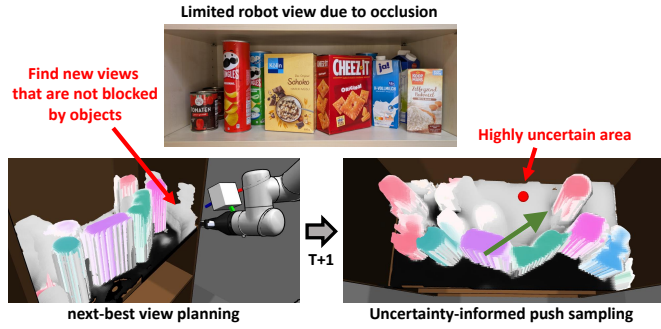


Fig. 1: The task of the robot is to map a shelf with dense clutter and heavy occlusions with its RGB-D sensor mounted on the arm. Highly uncertain areas are marked in white in the belief map whereas solid colors indicate low semantic uncertainty regions. Initially, the arm finds the next-best view targeting the highly uncertain regions on the right. Once frontier objects are mapped, the belief map indicates uncertain regions behind the occluding Schoko cereal box and Cheezit box. The informed push sampler finds the target region to uncover (red dot) and identifies the cereal box as the best candidate for occlusion removal. The green arrow indicates the chosen push candidate to unveil the region.

in table-top clutter for object retrieval and action selection between grasping and pushing. However, these methods act in perceptually easy arrangements and do not consider uncertainty-awareness. Recently, Marques *et al.* [10] demonstrated that evidential networks can significantly improve *Manipulation-Enhanced Mapping* (MEM) in confined shelf spaces by integrating observation and manipulation networks that jointly predict post-action occupancy and semantic map beliefs. However, they do not leverage belief uncertainty for continuous action planning, thereby presenting several opportunities for performance improvement. Firstly, instead of fixed view points, continuous-space next-best view planning enables fine-grained sensor placements that reveal occluded regions more effectively. Secondly, instead of using a selection strategy that randomly samples push candidates, informed sampling can be used to select pushes based on their expected impact on hidden areas, improving planning efficiency and interaction safety. Finally, driving exploration with semantic uncertainty rather than occupancy entropy alone can improve both occupancy estimates and semantic scene understanding.

To tackle these challenges, in this paper, we build upon [10] and propose informed strategies for action sampling and selection in the MEM-task. In particular, we introduce a reinforcement learning (RL)-based continuous viewpoint planner that uses occupancy and semantic uncer-

tainty estimates from the predicted map to allow the agent to select next-best views that maximize expected information gain, enabling more efficient and targeted exploration. RL provides the flexibility to adapt to diverse, dynamic scenes while effectively balancing exploration and exploitation, capabilities that are difficult to achieve with heuristic methods, sampling-based planners, or POMDPs in high-dimensional spaces.

In addition, we present a novel uncertainty-informed push selection strategy that identifies objects with high potential to reduce occlusions in uncertain map regions. By predicting and selecting minimally invasive, high-impact manipulations, our system improves visibility while minimizing unnecessary or unsafe interactions.

Our experiments demonstrate that the proposed MEM planner outperforms prior approaches [10] in terms of map accuracy and action efficiency. Specifically, our system achieves higher semantic and occupancy mean Intersection-over-Union (mIoU) scores, reduces the number of required push actions, and lowers the total object displacement—while being significantly faster in planning both views and manipulations.

II. RELATED WORK

1) *Interactive Perception*: Recent interactive perception frameworks that integrate physical interactions into the perception loop have demonstrated significant improvements in robustness and accuracy over active perception alone. Murali *et al.* showed up to a 36% increase in object-pose estimation accuracy compared to an active-vision baseline in dense clutter [11]. Similarly, Yao *et al.* demonstrated that interactively manipulating leaves to infer the shape and position of fruits significantly improves the accuracy of these estimates [6]. Furthermore, interactive perception enables the autonomous, online construction of affordance-based scene representations without requiring predefined object models, allowing robots to adaptively learn and operate in open, dynamic environments [5]. However, these methods do not consider the problem of dense clutter and confined spaces and approaches to uncover them.

2) *Uncertainty-Aware Action Selection*: Uncertainty-aware action selection methods employ probabilistic models to inform perception and manipulation, yielding more efficient and reliable task execution than heuristic-driven strategies. ActNeRF [12] uses an ensemble of NeRF models to quantify 3D reconstruction uncertainty and choose the next-best visual or reorientation action, accelerating object modeling under occlusions compared to random or greedy approaches. Furthermore, for mobile manipulation in unstructured settings, uncertainty can be used to adaptively select between sensing and manipulation actions that minimize environmental and sensory uncertainty [13]. Uncertainty-aware manipulation planning frameworks that represent object pose as probability distributions can systematically sequence pushes, placements, and grasps to eliminate pose ambiguity, achieving higher assembly success rates than deterministic planners [14].

Recently, evidential neural networks [15] have been increasingly deployed to estimate in a single forward pass, both aleatoric and epistemic uncertainties, guiding action selection in perception and manipulation. vMF-Contact [16] applies evidential learning with von Mises–Fisher models for grasping in cluttered environments, while Durasov *et al.* [17] leverages a Dirichlet-based evidential loss on bird’s-eye-view representations for 3D object detection to identify out-of-distribution objects and boost detection performance.

3) *Manipulation-Enhanced Mapping*: Robotic mapping in densely cluttered environments requires strategic perception, deciding *where* to observe, and proactive interaction, deciding *how* to manipulate occluding objects. Classical mechanical-search approaches leverage semantic relationships to guide push-and-pick actions for target retrieval [18], [3], [19]. Interactive mapping paradigms extend this idea, using manipulation primitives to resolve occlusions and complete spatial reconstructions. Wang *et al.* [20] build an actionable 3D relational object graph to perform targeted interactions to explore hidden regions in mobile settings. In the domain of cluttered confined spaces, such as shelves, Dengler *et al.* [4] proposed a deep RL framework that alternates viewpoint planning with push-action sampling on saturation of the marginal map entropy reduction. More recently, Marques *et al.* [10] adapted this idea and defined a POMDP solver whose belief resides in a metric-semantic grid map, with evidential neural-accelerated belief updates to reason about object shapes and manipulation consequences, achieving substantial gains in map accuracy.

Our work builds on these lines of research by leveraging the uncertainty estimates for occupancy and semantic prediction modeled using evidential networks [15] for learned continuous-space viewpoint planning and informed occlusion-critical push sampling, rather than random sampling or push-scoring networks [4]. Compared to prior MEM [10], our method concentrates exploration on regions with maximum expected information gain, reduces redundant manipulations, and lowers planning overhead—enabling online semantic mapping in cluttered, dynamic scenes.

III. OUR APPROACH

In this work, we address manipulation-enhanced mapping (MEM) of cluttered shelf environments using a robotic arm with a wrist-mounted RGB-D sensor. An illustration of our pipeline is shown in Fig. 2. Building on the evidential metric-semantic mapping of Marques *et al.* [10] via Calibrated Neural-Accelerated Belief Update (CNABU) networks, we fuse depth and RGB-D images into occupancy (Beta) and semantic (Dirichlet) maps, where each belief distribution inherently encodes both the predicted outcome and the associated uncertainty. An **next-best view RL-policy** (orange) then selects $SE(3)$ camera poses to observe regions of high-uncertainty. As pure active sensing exhibits submodular returns, when its expected volumetric information gain falls below a threshold, an **uncertainty-informed push selection** module (blue) identifies occlusion-critical objects via distance and visibility transforms, samples

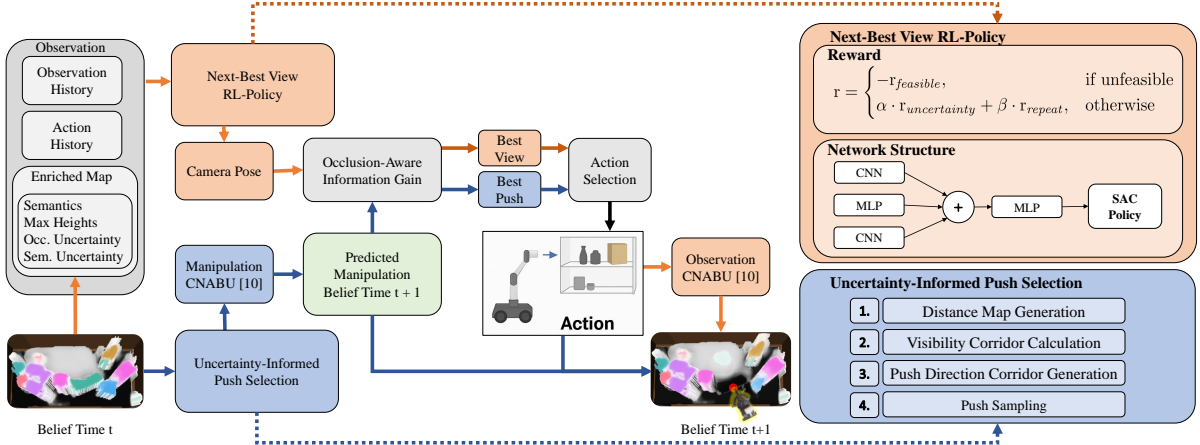


Fig. 2: Overview of our uncertainty-aware manipulation-enhanced mapping framework. Our system integrates evidential semantic mapping with a reinforcement learning (RL) policy for continuous viewpoint planning (orange) and a strategic, uncertainty-informed push module (blue). The RL agent operates in a 6D action space, leveraging uncertainty estimates from Beta and Dirichlet distributions to guide exploration towards occluded and ambiguous regions. When passive observation yields insufficient information gain, an informed manipulation policy selects occlusion-critical pushes to reveal hidden areas.

minimally invasive pushes, and evaluates their information gain. Finally, the **action selection** module (grey) chooses between sensing and manipulation based on their respective expected information gains, iterating until the mapping objective is achieved. The individual parts of our system are now introduced in detail.

A. Map Belief Representation

Accurate decision-making in MEM-tasks relies on reasoning about both observations and confidence. Following the CNABU framework [10], we represent the map belief as a probabilistic estimate over occupancy and semantic categories, enriched with explicit uncertainty. CNABU networks are designed to perform belief propagation in metric-semantic maps by predicting both semantic and occupancy beliefs, along with well-calibrated uncertainty estimates. They incorporate prior knowledge about object geometry, occlusions, and manipulation dynamics, enabling reliable forecasting of scene changes due to both observations and physical interactions. The occupancy belief is a 3D voxel map of size $H \times W \times D$, where each voxel is parameterized by $\lambda^O = (\alpha, \beta)$ and modeled by a Beta distribution whose predictive mean $\mathbb{E}[\text{Beta}(\alpha, \beta)]$ is the expected occupancy probability and whose variance

$$u_o = \text{Var}[\text{Beta}(\alpha, \beta)]$$

quantifies epistemic uncertainty. The semantic belief is a 2D top-down projected map of size $H \times W$ with evidential parameters $\lambda^S \in \mathbb{R}^{H \times W \times N_{\text{classes}}}$, where $\lambda_{i,j}^S = (\lambda_1, \dots, \lambda_N)$ defines a Dirichlet distribution whose predictive class probabilities

$$\mathbb{E}[\text{Dir}(\lambda_1, \dots, \lambda_N)]_n = \frac{\lambda_n}{S}, \quad S = \sum_{n=1}^N \lambda_n,$$

yield a hard label $\arg \max_n(\frac{\lambda_n}{S})$, and whose uncertainty

$$u_s = \frac{N}{S}$$

highlights low-confidence regions [15]. In our framework, both u_o and u_s guide action selection to maximize expected information gain.

B. Next-Best View Selection

To achieve effective scene coverage, we integrate the predictive capabilities of CNABU networks to estimate the map for the next time step [10] with a reinforcement learning (RL) agent that operates directly on the resulting evidential map representations. Our RL-agent receives as input both the occupancy and semantic beliefs, along with their corresponding uncertainty estimates. By explicitly leveraging these uncertainty measures, the agent is guided toward viewpoints that are expected to maximize information gain. In the following, we detail the architecture and training procedure of the RL-based viewpoint planner.

1) **Action:** We define the action space as a 6D vector $(x_{\text{cam}}, y_{\text{cam}}, z_{\text{cam}}, \text{target}_x, \text{target}_y, \text{target}_z)$, with each component normalized to $[-1, 1]$. At execution time these values are rescaled to predefined physical limits in $\text{SE}(3)$. We represent orientation implicitly via a look-at target to ensure the camera faces the region of interest (RoI), i.e., the shelf board.

2) **Observation:** Our observation space is detailed in Tab. I and it supports two key objectives:

(i) **Enhanced world representation:** As described in Sec. III-A, the agent’s world representation comprises of the 3D occupancy and 2D semantic belief maps. We project the thresholded occupancy belief into a 2D maximum-height map to reduce memory and computation while preserving occlusion reasoning and visibility assessment. Additionally, we incorporate cell-wise occupancy and semantic uncertainties, i.e., u_o and u_s , from the Beta and Dirichlet distributions to enable the agent to learn how its actions affect scene uncertainty.

(ii) **Action history awareness:** To avoid redundant observations and encourage coverage diversity, the observation space

TABLE I: Observation space used by the RL agent.

Component	Content	Shape
Enriched Map	Maximum Height	82 × 157px
	Semantic	82 × 157px
	Occupancy uncertainty u_o	82 × 157px
	Semantic uncertainty u_s	82 × 157px
Height Map History	Past normalized height maps	$N_{\text{hist}} \times 82 \times 157\text{px}$
Action History	Past normalized actions	$N_{\text{hist}} \times 6$

includes the last N_{hist} executed actions along with their corresponding 2D height map observations. This temporal context helps the agent identify previously explored areas and prioritize novel or more informative viewpoints.

3) **Reward**: The reward function comprises three terms:

$$r = \begin{cases} -r_{\text{feasibility}}, & \text{if unfeasible} \\ \alpha \cdot r_{\text{uncertainty}} + \beta \cdot r_{\text{repeat}}, & \text{otherwise} \end{cases} \quad (1)$$

Given the continuous nature of the action space, sampled actions may be infeasible for execution. Hence, during training, we use the Klamp't motion planning library [21] to check for action feasibility. For infeasible actions, the agent is penalized via a negative sparse reward signal $r_{\text{feasibility}}$ and an empty partial observation is returned in the observation space to reflect the failed attempt.

As **continuous reward** signals, we use the change in occupancy and semantic uncertainty $r_{\text{uncertainty}} = \Delta u_o + \Delta u_s$ between two time steps. Additionally, we use a repetition penalty r_{repeat} , which penalizes viewpoints close in position or orientation to previously visited ones [22]. In particular, r_{repeat} is computed as follows:

$$r_{\text{repeat}} = - \sum_{(p_{\text{past}}, e_{\text{past}}) \in \mathcal{H}} \left(\gamma_p \frac{\theta_p - p_{\text{dist}}}{\theta_p} + \gamma_e \frac{\theta_e - e_{\text{dist}}}{\theta_e} \right), \quad (2)$$

$$p_{\text{dist}} = \|p_{\text{curr}} - p_{\text{past}}\|, \quad e_{\text{dist}} = \|e_{\text{curr}} - e_{\text{past}}\|, \quad (3)$$

Here, p_{dist} and e_{dist} denote the Euclidean distance between positions and the cosine distance between the rotation vectors, respectively, within the action history stack \mathcal{H} . The terms γ_p and γ_e are scaling factors, while θ_p and θ_e are the corresponding distance thresholds. The repetition penalty r_{repeat} is computed only for entries in \mathcal{H} where $p_{\text{dist}} \leq \theta_p$ and $e_{\text{dist}} \leq \theta_e$.

C. Push Sampling

To enhance visibility and maximize information gain in cluttered and confined environments, particularly when only executing observations proves insufficient, we leverage strategic uncertainty-aware object manipulation to uncover occluded regions. In the following, we detail the process of identifying suitable manipulation targets, estimating visibility corridors, determining effective push directions, and finally sampling feasible push interactions. An illustration of each step is shown in Fig. 3.

1) **Target Locations**: Unlike existing object-search methods [23], [3], we define target locations as regions of the map with high semantic uncertainty. We prioritize semantic uncertainty over occupancy uncertainty because even when occupancy estimates are confident, class labels can remain ambiguous. Focusing on semantics drives the robot

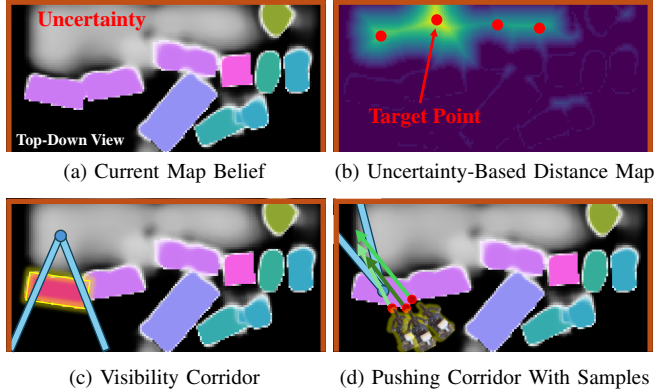


Fig. 3: Uncertainty-informed push sampling. From the current map belief (a), with shelf borders indicated in brown, we generate target points from a distance map representing the occupancy uncertainty-weighted distance to the nearest confidently classified cell (b). Then, we compute visibility corridors using raycasting from each target location to the front of the shelf, identifying occluding objects, as highlighted in yellow for one of the corridors (c). Finally, n_p push proposals are sampled from feasible start regions along the identified occluding object, aligned with pushing corridors, that represent the best direction for the object to be pushed into (d). The generated push samples are used as input to the manipulation CNABU to evaluate their expected information gain.

to discover new objects and improve its understanding of known ones. To identify these regions, we compute a distance transform over a thresholded version of the semantic uncertainty, where cells with a semantic uncertainty below 0.1 are considered sufficiently certain and set to 0. The distance transform assigns each cell a score based on how far it is from the nearest confidently classified cell (either free or occupied), with the score scaled by cells occupancy uncertainty value. From the resulting distance map, the n_p maximum offive cells with the highest distance values are selected as candidate target locations, while ensuring a minimum pairwise distance to promote spatial diversity as highlighted in Fig. 3b.

2) **Visibility Corridor**: For each selected target location, a visibility corridor is constructed to identify potential occlusions. This is accomplished using raycasting, from the target point 180 degrees toward the front of the shelf, recording the number of semantic object instances from the one-hot-encoded map that are encountered along the ray as well as the average occupancy probability weighted by the epistemic occupancy uncertainty. Neighboring rays that exhibit similar spatial structures (in terms of object instances and non-occupied space) are clustered into unified corridors up to a maximum radius of n_c cells. These corridors are scored according to four criteria:

$$\text{score} = k_1 \cdot w + k_2 \cdot l + k_3 \cdot \bar{p}_{\text{occ}} + k_4 \cdot n_{\text{occ_obj}} \quad (4)$$

where w is the width of the corridor, l the length of the visibility corridor, \bar{p}_{occ} the average occupancy probability, $n_{\text{occ_obj}}$ the number of occluding objects, and $k_{1,2,3,4}$ are weights. The object closest to the front of the shelf within the corridor with the highest score is selected as the manipulation target (see Fig. 3c). Note that if no occluding object is found,

the target is considered observable through future viewpoint planning and no push is considered.

3) **Pushing Corridor:** The objective is to find a direction that minimizes secondary pushing of adjacent objects and prefers already mapped free areas over highly uncertain ones. Therefore, unlike the visibility corridor, sectors with lower average occupancy and greater clearance are preferred to ensure good reachability and low collision probabilities with other objects. To determine viable pushing directions for the selected object, again raycasting is employed. Rays are radially cast from the centroid of the object identified as pushing target toward a circular boundary with a maximum radius of n_c cells. We identify object entities and their centroids by clustering connected regions of similar semantic labels in the current map. For each object, we cast rays from its centroid inside the shelf in multiple directions, grouping these rays into sectors with a maximum angle of 30 degrees. Each sector is evaluated based on the average occupancy along its rays and spatial constraints such as nearby obstacles or shelf boundaries (see Fig. 3d, blue corridor).

4) **Sampling Push Interactions:** To generate possible pushes to execute, a starting corridor is established on the side opposite the pushing corridor (see Fig. 3d). This is achieved by identifying a wider region on the object's contour based on the intersection points of lines defined by the endpoints of both corridors.

Within this starting region, n_p candidate push points are uniformly sampled. The associated push direction is computed as a linear combination of the pushing corridor vectors, weighted according to the relative position of each sampled point. Generating the push proposals in this fashion, results in feasible minimally invasive push actions aligned with free-space directions.

D. Manipulation-Enhanced Planning

We combine our viewpoint selection policy with the uncertainty informed push-based manipulation strategy to realize a complete manipulation-enhanced mapping pipeline. While the RL-based next-best view (NBV) planning agent seeks to maximize information gain through passive camera movement, physical occlusions can make certain regions permanently inaccessible to observation. In such cases, the system queries the push sampling module to actively remove occlusions.

For decision making, we employ a variant of the occlusion-aware Volumetric Information Gain (VIG) planning strategy proposed by [10]. For the NBV module, we query the trained RL agent to generate a single candidate action, obtain the predicted camera pose, and compute the associated VIG based on the evidential occupancy prediction at time $t - 1$. Similarly, for the push sampling module, we simulate the outcome of each push by generating its parameterization and input it together with the evidential occupancy prediction at time $t - 1$ to the manipulation-CNABU to predict the resulting updated evidential map. Subsequently, we query the NBV agent on the post-push

map, incorporating the effects of the simulated manipulation, and compute the corresponding VIG.

The system then compares the maximum expected VIG from viewpoint planning (VIG_{nbv}) against that from push actions (VIG_{push}). If the VIG achievable through viewpoint selection exceeds that of any proposed push by a predefined margin $VIG_{nbv} \cdot \Delta_{view} > VIG_{push}$, the system executes the corresponding NBV action. Otherwise, if pushing is expected to yield higher information gain, the robot proceeds to execute the selected push to actively modify the scene and takes its predicted belief generated by the manipulation-CNABU as map representation. [TODO: does an observation action follow or not? This is also unclear from Fig 2]

This strategy ensures that executing viewpoints is always prioritized when sufficient information gain can be achieved without manipulation, while empowering the system to physically interact with the environment whenever necessary to uncover previously inaccessible regions and maximize overall map accuracy.

IV. EXPERIMENTAL EVALUATION

We perform three experimental evaluations to showcase the performance of our next-best view and push selection approach. First, we present quantitative simulation results that highlight our pipeline's improvements in mapping accuracy, compared to the state-of-the-art for manipulation-enhanced mapping [10]. Next, we present several ablations of our method to highlight the influence of uncertainty measurements for action selection and evaluate different versions of our novel push sampling strategy. Finally, we show a qualitative experiment in a real hardware setup in zero-shot fashion in the supplementary video.

A. Experimental Setup and Training

For simulation, we use the PyBullet physics engine [24] with a 6-DOF UR5 robotic arm, equipped with a Robotiq 2F-85 gripper and a Realsense L515 RGB-D camera mounted on its end-effector. The simulation matches the real-world camera parameters and all experiments are trained and evaluated on an NVIDIA RTX 4080 Super 16GB GPU. To train the continuous viewpoint planning agent, we use the Soft Actor-Critic (SAC) algorithm [25], implemented via the Stable Baselines3 framework [26].

For the actor and critic networks, we use the following custom feature extractor: (i) A convolutional encoder for the enriched map, consisting of three convolutional layers with 16, 32, and 64 filters, each followed by LeakyReLU activation, with the last layer performing global average pooling and flattening. (ii) A similar encoder for the stacked height maps. (iii) A fully connected module embedding the last four actions into a vector of size 64. The outputs are concatenated and passed through an MLP, projecting it to a 128-dimensional latent space, feeding both policy and critic heads. Training uses a batch size of 256, a replay buffer of 10^5 transitions, and a learning rate of $3 \cdot 10^{-4}$.

The agent is trained for 500,000 iterations across approximately 12,500 procedurally generated shelf configurations.

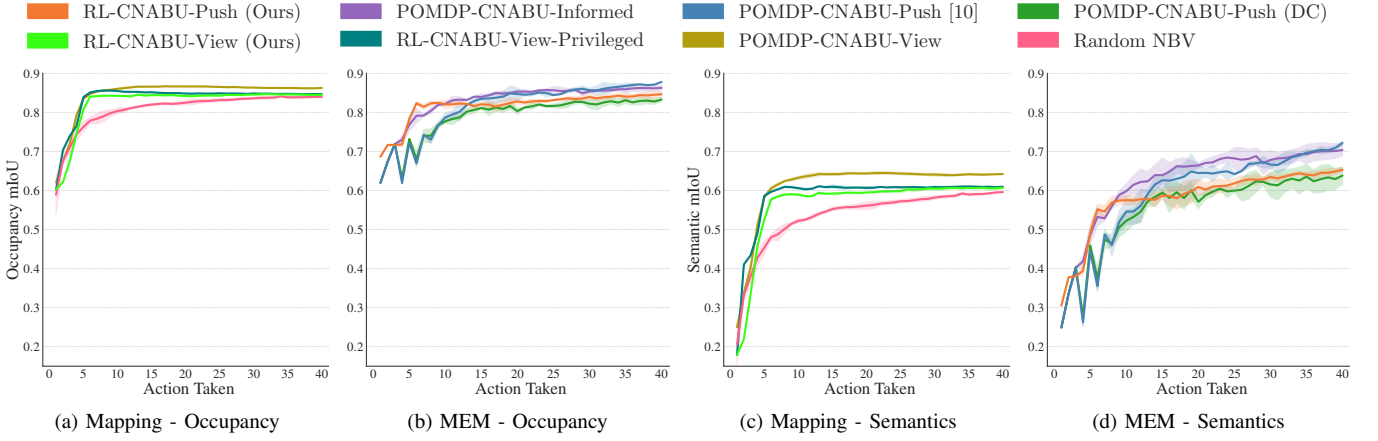


Fig. 4: Simulation results across 25 highly cluttered shelf environments with an action budget of 40 steps for RL-CNABU-Push and RL-CNABU-View against SOTA in active and interactive perception methods, showing both occupancy and semantic IoUs over time for each method. Standard deviation is represented as shading around each plot. As can be seen, our uncertainty-informed push strategy, POMDP-CNABU-Informed, outperforms previous work in terms of stable mapping without object drops. Furthermore, our proposed RL-CNABU-View is capable of achieving sufficient mapping behaviour without relying on privileged knowledge.

Model	Perception	Push Strategy	Occ. mIoU \uparrow	Sem. mIoU \uparrow	mAD [m] \downarrow	NumPush [#] \downarrow	Collisions [%] \downarrow
RL-CNABU-View (Ours)	Active	None	0.844 \pm 0.001	0.607 \pm 0.002	-	-	-
RL-CNABU-View-Privileged	Active	None	0.846 \pm 0.001	0.609 \pm 0.002	-	-	-
POMDP-CNABU-View [10]	Active	None	0.862 \pm 0.001	0.641 \pm 0.001	-	-	-
Random-View	Active	None	0.839 \pm 0.002	0.595 \pm 0.001	-	-	-
RL-CNABU-Push (Ours)	Interactive	$u_s u_o$	0.846 \pm 0.007	0.653 \pm 0.005	0.995 \pm 0.049	2.59 \pm 1.24	6.67%
POMDP-CNABU-Push [10]	Interactive	Random Sampling	0.877 \pm 0.003	0.720 \pm 0.019	1.927 \pm 0.046	5.25 \pm 2.61	25.33%
POMDP-CNABU-Push (DC)	Interactive	Random Sampling	0.832 \pm 0.005	0.638 \pm 0.022	1.841 \pm 0.033	4.65 \pm 2.50	25.33%
POMDP-CNABU-Informed	Interactive	$u_s u_o$	0.862 \pm 0.006	0.703 \pm 0.015	1.056 \pm 0.157	2.61 \pm 1.49	6.67%
POMDP-CNABU-Informed	Interactive	$u_o u_o$	0.862 \pm 0.005	0.698 \pm 0.012	1.060 \pm 0.255	2.91 \pm 1.24	9.33%

TABLE II: Quantitative comparison over 25 cluttered scenes, averaged across three trials. We report occupancy and semantic mIoU, mean action displacement (mAD), push count, and collision rate. Our informed strategies ($u_s|u_o$, $u_s|u_b$, $u_o|u_o$) and RL-based methods show benefits of uncertainty-aware action selection. While POMDP-CNABU-Push achieves the highest semantic mIoU, it does so at the cost of more frequent pushing and a high collision rate. In contrast, our RL-CNABU-Push approach offers a better balance, achieving competitive mapping performance with fewer pushes, lower movement, and reduced number of collisions.

Object counts range from 15 to 30 per scene. To simulate varying occlusion levels for training, large objects are biased toward the front of the shelf and smaller ones toward the back, increasing visual complexity. The action space is sampled from a Cartesian space of $0.8\text{ m} \times 0.2\text{ m} \times 0.2\text{ m}$ outside and inside the shelf, respectively.

The following hyperparameters are used for all experiments: $N_{\text{hist}} = 4$, $\Delta_{\text{view}} = 2$, $\theta_{\text{sem}} = 0.65$, and $\theta_{\text{occ}} = 0.87$. For the reward function of the viewpoint planning agent, we set $\alpha = 10$ and $\beta = 2$.

B. Metrics and Baselines

To evaluate our informed action selection pipeline for the given MEM-task, we evaluate the following metrics for semantic and occupancy accuracy, object displacement, and pipeline efficacy:

- **mIoU:** Semantic and occupancy mean Intersection-over-Union.
- **mAD:** Mean displacement of each object averaged over all evaluated scenes.
- **NumPush:** Average number of pushes per scene.
- **Timings:** Inference and execution timings of the pipelines

Furthermore, we compare our **full system RL-CNABU-Push (Ours)** against the following baselines and state-of-the-art:

- **RL-CNABU-View (Ours):** Uncertainty-aware RL based next-best-view (NBV) planner.
- **RL-CNABU-View-Privileged (Ours):** RL based NBV planner that uses ground truth occupancy and semantics from privileged simulation information for rewards.
- **Random-View:** View planner that randomly selects sensor poses from the RL action space.
- **POMDP-CNABU-Push:** Full pipeline by Marques *et al.* [10] that uses a partially observable Markov decision process (POMDP) two-step look-ahead solver with randomly sampled push actions.
- **POMDP-CNABU-Push (DC):** POMDP-CNABU-Push terminated when any of the objects drop down.
- **POMDP-CNABU-View:** Only NBV planning by [10].
- **POMDP-CNABU-Informed:** Pipeline [10] with novel push sampling (see Sec. III-C).

For each method, we perform three evaluation trials and report the mean and the standard deviation.

C. Quantitative Experiments

We present our quantitative experiments, designed to evaluate the effectiveness of our proposed manipulation-enhanced mapping pipeline. To compare our approach against POMDP-CNABU planners, we re-implemented their pipeline and used the provided CNABU-models from their code release. In order to use the models for our approach,

no fine-tuning on the novel set of continuous viewpoints was performed. However, we increased the certainty threshold for full map completion after which no pushes are performed from 95%, as stated in [10], to 99%. This increases the chance of further pushes in the long run and shows the effect of successful push prediction on the over- or under-confidence of the CNABU-models.

1) **Timings:** We evaluate the computational efficiency of our methods against the POMDP-CNABU baselines. As shown in Table III, our method significantly reduces decision latency in both viewpoint and manipulation selection. This is primarily due to our reinforcement learning-based viewpoint planner, which operates in a continuous action space and avoids exhaustive enumeration and ray-casting of discrete candidates, as well as our informed push sampling strategy, which narrows down the set of evaluated push actions while preserving their impact on map improvement. In particular, our **RL-CNABU-View** planner achieves a **99.7%** reduction in average inference time per step compared to the original **POMDP-CNABU-View** planner. Similarly, the informed push selection time and the total per-iteration execution times are significantly reduced, enabling faster scene coverage and improved responsiveness.

2) **Map Quality:** To assess the effectiveness of our proposed system in building complete and accurate scene representations, we evaluate semantic and occupancy map quality across 25 highly cluttered shelf environments with an action budget of 40 steps and evaluate them according to the metrics specified in Sec. IV-B. The results across the whole action budget is illustrated in Fig. 4 with a more detailed analysis of the last step shown in Tab. II. In the following, we summarize the main results.

Among active perception methods, although **POMDP-CNABU-View** performs better than **RL-CNABU-View** in mapping accuracy, it highly relies on the quality of the predefined fixed views and is computationally expensive as it uses a greedy search over up to 300 fine-tuned views, querying expected information gain at each step. In contrast, our **RL-CNABU-View** predicts the next-best view with a single forward pass through a learned continuous-space policy, substantially reducing computation time while maintaining comparable mIoU. With regards to active versus interactive perception, Tab. II shows that the worst performing interactive perception method achieves higher semantic mIoU than the best active perception method, highlighting the need for physical interaction. In particular, our uncertainty-informed push method, **RL-CNABU-Push** achieves higher semantic mIoU than both **RL-CNABU-View** and **POMDP-CNABU-View**, demonstrating that targeted push actions can improve mapping accuracy by uncovering hidden regions. For interactive perception, Fig. 4 and Tab. II show that **POMDP-CNABU-Push** achieves higher mIoU metrics compared to **RL-CNABU-Push**. However, unlike all other methods, this proposed pipeline [10] does not consider any early stopping when an object drops, e.g., out of the shelf, due to collisions. As can be seen, when terminating after

Metric	POMDP-CNABU-Push	RL-CNABU-Push
View Point Selection Time (s)	7.632 ± 1.892	0.022 ± 0.001
Push Selection Time (s)	31.199 ± 7.814	0.976 ± 0.618
Full Iteration Time (s)	40.093 ± 10.095	1.656 ± 1.117

TABLE III: Timing performance in seconds across the 25 evaluation scenes averaged over 40-step rollouts and across three trials. Our RL and uncertainty aware push approach highly reduces the individual and overall inference time of the task.

an object drop occurred, our proposed **RL-CNABU-Push** achieves better occupancy and semantic mIoU compared to **POMDP-CNABU-Push** (DC).

As all POMDP-CNABU-Push variants use random push sampling to generate pushes without knowledge of effective pushing corridors, they result in the highest mean displacement and collision rates among interactive perception methods. In **POMDP-CNABU-Informed**, replacing random sampling with our uncertainty-informed strategy increases mIoU while significantly reducing average displacement, number of pushes, and collisions. The reduced displacement and collisions in all the informed push methods confirm that our interactions are minimally invasive compared to the random push sampling baseline. Furthermore, informed push sampling methods require only 2–3 pushes versus 4–5 in random methods to achieve comparable or better map quality, demonstrating more targeted uncovering of hidden spaces.

These results confirm that leveraging epistemic uncertainty for both viewpoint and manipulation planning leads to comparable or better quality map quality, particularly in scenes with high occlusion. Furthermore, as the timing results indicate our method achieves comparable mapping accuracy and reliability, with significantly better computational efficiency

D. Influence of Uncertainty

To assess the influence of uncertainty metrics on the action selection process, we perform two ablation studies.

1) **Next-Best View planning:** We evaluate our uncertainty-aware agent **RL-CNABU-View** against **RL-CNABU-View-Privileged**, which incorporates ground-truth occupancy and semantics into its reward, using the same test set as in Sec. IV-C.2. We adopt the reward $r = r_{\text{IoU}} + r_{\text{repeat}}$, where r_{IoU} is the change in semantic and occupancy IoU from the ground-truth map. This ablation shows that uncertainty-based rewards suffice to learn effective next-best view selection without privileged information. We also compare our **RL-CNABU-View** method to **Random-View** to verify that our RL agent learns informative views.

As shown in Fig. 4.a,c, our reward achieves similar or only slightly reduced long-term performance compared to the privileged agent. These findings demonstrate that uncertainty is a reliable performance proxy when ground-truth data is unavailable. Moreover, Random-View shows lower occupancy and semantic mIoU gains in the initial phases in Fig. 4, with the final mapping accuracy also the lowest among all active perception methods. Overall, our RL agent attains higher IoU, confirming its learned ability to select informative views.

2) **Manipulation:** To evaluate the influence of different uncertainty representations on our push sampling strategy, we conduct ablation experiments with two variants for distance map and pushing corridor generation: **(i)** using semantic uncertainty for distance map generation while using occupancy uncertainty for the pushing corridor ($u_s|u_o$) to highlight semantically ambiguous but structurally visible regions, providing complementary cues for selecting informative push targets, the proposed method of this paper; and **(ii)** using occupancy uncertainty for both the uncertainty-based distance map and the pushing corridor generation ($u_o|u_o$). We performed this ablation on the **POMDP-CNABU-Informed** push planner to have a more comparable evaluation that only focuses on the influence of the push selection, due to its systematic greedy search characteristics of the predefined fixed viewpoints.

The results after the final action step are presented in Tab. II. As seen from the last two rows, using u_s as the base for distance map yields marginally higher semantic mIOU as it is better able to target regions with high semantic uncertainty. Furthermore, it leads to lower collision rates possibly due to clustering of semantically similar cells leading to pushes being executed on single objects reducing secondary pushes.

Our ablation studies on uncertainty metrics' influence show that uncertainty is a good proxy for action selection between active sensor placement and manipulation. While semantic uncertainty can be used to target regions for active observation as well as for the push distance map, occupancy uncertainty can be effectively used to generate minimally invasive push actions.

V. CONCLUSION

In this paper, we presented a novel framework for efficient manipulation-enhanced semantic mapping that combines evidential metric-semantic map belief updates with uncertainty-aware action selection. By leveraging uncertainty estimates derived from the Beta and Dirichlet distributions, our system effectively selects informative next-best views through reinforcement learning and targets occlusion-critical objects for minimally invasive manipulations. Our integrated framework enables a robot to construct complete semantic maps in cluttered, occlusion-heavy shelf environments.

We demonstrated that our uncertainty-informed push planning approach outperforms the state-of-the-art method in terms of map accuracy, object displacement, and action efficiency. Furthermore, our approach is computationally efficient due to the reinforcement learning based viewpoint planning, and the informed push sampling strategy. These results highlight the importance of principled uncertainty-informed action selection for interactive perception in cluttered and confined spaces.

REFERENCES

- [1] N. O’Mahony, S. Campbell, L. Krpalkova, D. Riordan, J. Walsh, A. Murphy, and C. Ryan, “Computer vision for 3d perception: A review,” in *Intelligent Systems and Applications: Proceedings of the 2018 Intelligent Systems Conference (IntelliSys)*, 2019.
- [2] H. Jiang, B. Huang, R. Wu, Z. Li, S. Garg, H. Nayyeri, S. Wang, and Y. Li, “Roboexp: Action-conditioned scene graph via interactive exploration for robotic manipulation,” *Proc. of Conf. on Robot Learning (CoRL)*, 2024.
- [3] H. Huang, L. Fu, M. Danielczuk, C. M. Kim, Z. Tam, J. Ichnowski, A. Angelova, B. Ichter, and K. Goldberg, “Mechanical search on shelves with efficient stacking and destacking of objects,” in *The International Symposium of Robotics Research*. Springer, 2022.
- [4] N. Dengler, S. Pan, V. Kalagaturu, R. Menon, M. Dawood, and M. Bennewitz, “Viewpoint push planning for mapping of unknown confined spaces,” in *Proc. of the IEEE/RSJ Intl. Conf. on Intelligent Robots and Systems (IROS)*, 2023.
- [5] T. Engelbracht, R. Zurbrügg, M. Pollefeys, H. Blum, and Z. Bauer, “Spotlight: Robotic scene understanding through interaction and affordance detection,” *arXiv preprint arXiv:2409.11870*, 2024.
- [6] S. Yao, S. Pan, M. Bennewitz, and K. Hauser, “Safe leaf manipulation for accurate shape and pose estimation of occluded fruits,” in *Proc. of the IEEE Intl. Conf. on Robotics & Automation (ICRA)*, 2025.
- [7] Y. Miao, R. Wang, and K. Bekris, “Safe, occlusion-aware manipulation for online object reconstruction in confined spaces,” in *The International Symposium of Robotics Research*. Springer, 2022.
- [8] B. Tang and G. S. Sukhatme, “Selective object rearrangement in clutter,” in *Conference on Robot Learning*. PMLR, 2023, pp. 1001–1010.
- [9] B. Huang, S. D. Han, J. Yu, and A. Boularias, “Visual foresight trees for object retrieval from clutter with nonprehensile rearrangement,” *IEEE Robotics and Automation Letters (RA-L)*, vol. 7, no. 1, pp. 231–238, 2021.
- [10] J. M. C. Marques, N. Dengler, T. Zaenker, J. Muecke, W. Shenlong, M. Bennewitz, and K. Hauser, “Map space belief prediction for manipulation-enhanced mapping,” 2025.
- [11] P. K. Murali, A. Dutta, M. Gentner, E. Burdet, R. Dahiya, and M. Kaboli, “Active visuo-tactile interactive robotic perception for accurate object pose estimation in dense clutter,” *IEEE Robotics and Automation Letters (RA-L)*, 2022.
- [12] S. Dasgupta, A. Gupta, S. Tuli, and R. Paul, “Actnerf: Uncertainty-aware active learning of nerf-based object models for robot manipulators using visual and re-orientation actions,” in *Proc. of the IEEE/RSJ Intl. Conf. on Intelligent Robots and Systems (IROS)*, 2024.
- [13] M. Tzes, V. Vasilopoulos, Y. Kantaros, and G. J. Pappas, “Reactive informative planning for mobile manipulation tasks under sensing and environmental uncertainty,” in *Proc. of the IEEE Intl. Conf. on Robotics & Automation (ICRA)*, 2022.
- [14] F. von Drigalski, K. Kasaura, C. C. Beltran-Hernandez, M. Hamaya, K. Tanaka, and T. Matsubara, “Uncertainty-aware manipulation planning using gravity and environment geometry,” *IEEE Robotics and Automation Letters (RA-L)*, 2022.
- [15] M. Sensoy, L. Kaplan, and M. Kandemir, “Evidential deep learning to quantify classification uncertainty,” *Advances in neural information processing systems*, 2018.
- [16] Y. Shi, E. Welte, M. Gilles, and R. Rayyes, “vmf-contact: Uncertainty-aware evidential learning for probabilistic contact-grasp in noisy clutter,” *Proc. of the IEEE Intl. Conf. on Robotics & Automation (ICRA)*, 2025.
- [17] N. Durasov, R. Mahmood, J. Choi, M. T. Law, J. Lucas, P. Fua, and J. M. Alvarez, “Uncertainty estimation for 3d object detection via evidential learning,” *arXiv preprint arXiv:2410.23910*, 2024.
- [18] S. Sharma, H. Huang, K. Shivakumar, L. Y. Chen, R. Hoque, brian ichter, and K. Goldberg, “Semantic mechanical search with large vision and language models,” in *7th Annual Conference on Robot Learning*, 2023.
- [19] M. Danielczuk, A. Kurenkov, A. Balakrishna, M. Matl, D. Wang, R. Martín-Martín, A. Garg, S. Savarese, and K. Goldberg, “Mechanical search: Multi-step retrieval of a target object occluded by clutter,” in *Proc. of the IEEE Intl. Conf. on Robotics & Automation (ICRA)*, 2019.
- [20] Y. Wang, L. Fermoselle, T. Kelestemur, J. Wang, and Y. Li, “Curiousbot: Interactive mobile exploration via actionable 3d relational object graph,” *arXiv preprint arXiv:2501.13338*, 2025.
- [21] K. Hauser, “Robust contact generation for robot simulation with unstructured meshes,” in *Proc. of the Intl. Symposium on Robotic Research (ISRR)*, 2013.
- [22] R. Menon, T. Zaenker, N. Dengler, and M. Bennewitz, “Nbv-sc: Next best view planning based on shape completion for fruit mapping and reconstruction,” in *Proc. of the IEEE/RSJ Intl. Conf. on Intelligent Robots and Systems (IROS)*. IEEE, 2023.

- [23] W. Bejjani, W. C. Agboh, M. R. Dogar, and M. Leonetti, “Occlusion-aware search for object retrieval in clutter,” in *Proc. of the IEEE/RSJ Intl. Conf. on Intelligent Robots and Systems (IROS)*, 2021.
- [24] E. Coumans and Y. Bai, “Pybullet, a python module for physics simulation for games, robotics and machine learning,” <http://pybullet.org>.
- [25] T. Haarnoja, A. Zhou, P. Abbeel, and S. Levine, “Soft actor-critic: Off-policy maximum entropy deep reinforcement learning with a stochastic actor,” in *Proc. of the Intl. Conf. on Machine Learning*, 2018.
- [26] A. Raffin, A. Hill, A. Gleave, A. Kanervisto, M. Ernestus, and N. Dormann, “Stable-baselines3: Reliable reinforcement learning implementations,” *Journal of Machine Learning Research*, 2021.